Penetration of external field into regular and random arrays of nanotubes: Implications for field emission

T. A. Sedrakyan, E. G. Mishchenko, and M. E. Raikh
Department of Physics, University of Utah, Salt Lake City, Utah 84112, USA
(Received 5 April 2006; published 20 June 2006)

We develop an analytical theory of polarization of a vertically aligned array of carbon nanotubes (NTs) in external electric field. Such arrays are commonly utilized in field-emission devices, due to the known electrostatic effect of strong field enhancement near the tip of an *individual* NT. A small ratio of the NT radius to the separation between neighboring NTs allows us to obtain asymptotically exact solution for the distribution of induced charge density along the NT axes. For a regular array, this solution allows us to trace the suppression of the field penetration with increasing the density of NTs in the array. We demonstrate that for a random array, fluctuations in the NT density terminate the applicability of our result at distances from the NT tips much larger than the field penetration depth, where the induced charge density is already exponentially small. Our prime conclusion is that, due to *collective* screening of the external field by the array, the field-emission current *decreases* drastically for dense arrays compared to an individual NT. We argue that the reason why the strong field emission, described by the Fowler-Nordheim law and observed in realistic arrays, is the strong dispersion in heights of the constituting NTs.

DOI: 10.1103/PhysRevB.73.245325 PACS number(s): 73.40.Gk, 79.70.+q, 79.60.Ht, 81.07.De

I. INTRODUCTION

The first report of field emission from carbon nanotubes (NTs) appeared a decade ago.[1] It was followed by a demonstration[2] that arrays of NTs can be patterned into emitting and nonemitting regions. Since then, the field emission properties of carbon NTs command a steady interest from researchers worldwide. The uniqueness of these properties originates from the geometry of a NT. Namely, due to a small NT radius, r, the electric field applied between the substrate (cathode), on which the NTs are grown, and the anode is enhanced by a large factor $\beta \gg 1$ near the nanotube tip. Such an enhancement translates into high probability of electron tunnelling toward the anode, leading to desirable low turn-on voltage for field emission. This property, combined with high emission current density, made possible a successful fabrication of the row-column matrix-addressable flat panel display based on carbon NTs.[3–11] Currently, flat panel displays constitute one of the most prominent applications of NTs.[12] Geometrical characteristics of individual NTs utilized in the first display[3] were highly dispersed. Further advances in fabrication[13] allowed the achievement of excellent vertical alignment and high homogeneity in the lengths and radii of NTs.[14–17] This suggests that NTs on the cathode of a display can, in the first approximation, be viewed as constituting a *regular array* of identical NTs. Such an array is schematically illustrated in Fig. 1.

On the theoretical side, the focus of the previous studies[18–27] of field emission from nanotubes was the effect of band structure and tip geometry of an *individual* NT on the emission probability. These studies left out the fact that *all* NTs are coupled to each other *electrostatically*.

The main point of the present paper is that, for a regular NT array, mutual electrostatic coupling of NTs in the array has a dramatic effect on the field emission, especially in dense arrays. By dense we mean the arrays in which the separation, d, between neighboring NTs is much smaller than the NT height, h. The situation $d \ll h$ is quite common in realistic field-emission setups, see, e.g., Refs. 15–17. To substantiate this point, consider first two parallel NTs separated by $d \ll h$ in the external electric field, F, directed along their axes (see Fig. 1). It might seem that if d exceeds the tunnelling length for field emission from each of the NTs, then both NTs emit independently. This, however, is not the case. The reason is that the enhancement of the electric field near the tip of each NT is governed by the charge density, induced by the external field. For two parallel NTs, the induced charge density *per* NT is approximately *two times smaller* than for an isolated NT.[28] As a result, the field enhancement near the tip of each NT becomes smaller due to the presence of the neighbor.

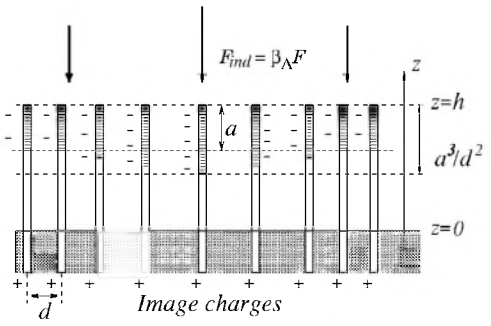

FIG. 1. Schematic illustration of the forest of NTs of a height, h, grown on the substrate, $z=0$. The average distance between neighboring NTs is d. Shaded regions at the NT tips illustrate the charges, induced in the NTs by the external field, F. For a dense forest, the typical penetration depth, a, exceeds d. Vertical arrows illustrate electric field, F_{ind}, created by induced charges. Regions of lower NT density correspond to higher field-enhancement-factor, $\beta_A = F_{ind}/F$. In these regions, the external field penetrates deeper into the forest. Fluctuations in the induced charge density, due to the randomness in the NT positions, exceed the average density at depth $(h-z) > a^3/d^2$.

Compared to a pair of neighboring NTs, the suppression of the field enhancement becomes much more pronounced *in the NT array*. On the qualitative level, this conclusion follows from the fact that each NT in the array interacts with $\sim(h/d)^2 \gg 1$ neighbors. As we will demonstrate below, the external field simply *does not penetrate* into the sufficiently dense array. On the intuitive level, this trend has been previously understood.[16,29,30] In particular, in Ref. 29 numerical simulations illustrating the suppression of the field enhancement for three parallel NTs with decreasing distance between them were reported. However, full understanding of this suppression *in the array* with arbitrary ratio d/h requires an analytical theory. Such a theory is developed in the present paper. In particular we demonstrate that

(*i*) penetration of the external field into the array is described by a simple function, $\sinh(z/a)$, where the penetration depth, a, is much smaller than h for a dense array, but still much bigger than d;

(*ii*) distributions of induced charge density in regular and completely random NT arrays are approximately *the same*;

(*iii*) with regard to the field emission, the enhancement of external field for the array, as compared to the individual NT, is suppressed by the factor $\approx(h/a)$.

The reason why the electrostatic problem, in which the variables cannot be separated, allows an asymptotic analytical solution is the presence of large parameters $(h/r) \gg 1$ and $(d/r) \gg 1$. As it was demonstrated in Ref. 31, for a single NT, the relation $h \gg r$ allows one to find analytically the distribution of induced charges in external field. Here the approach of Ref. 31 is generalized to the NT array.

The paper is organized as follows. In Sec. II we review the Thomas-Fermi description[31] of polarization of a single NT in external field. In Sec. III we generalize the Thomas-Fermi equation to the NT array. In Secs. IV and V we analyze this equation for a regular array, and find its asymptotic [in the parameter $(d/r) \gg 1$] solution. Robustness of this solution with respect to randomness in the NT positions is demonstrated in Sec. VI. In Sec. VII we apply to the obtained solution for distribution of the induced charge density to calculate the field emission current from the array. Relation of our theory to experiment is addressed in Sec. VIII.

II. SINGLE NT

Denote with $\rho(z)$ the *linear* charge density on the NT surface at a distance $z<h$ from the substrate. The Thomas-Fermi equation for $\rho(z)$ reads[31]

$$eFz = \frac{1}{g}\rho(z) + \frac{1}{e}\int_0^h dz' \mathcal{S}_0(z,z')\rho(z'), \tag{1}$$

where the kernel, $\mathcal{S}_0(z,z')$, is defined as

$$\mathcal{S}_0(z,z') = \Phi(z-z') - \Phi(z+z'). \tag{2}$$

Here the function $\Phi(z)$ is the interaction potential between two points on the NT surface, separated vertically by z. It represents an azimuthal average of the Coulomb potential

$$\Phi(x) = \frac{e}{\pi}\int_0^\pi \frac{d\alpha}{[x^2 + 4r^2\sin^2(\alpha/2)]^{1/2}}, \tag{3}$$

where r is the NT radius. The second term in Eq. (2) accounts for the image charges. The meaning of Eq. (1) is the following. The left hand side (lhs) is the bare potential. The potential, acting on a given electron at the NT surface, represents the sum of this potential and of the potential created by the induced charges. This resulting potential defines the *local* value of the Fermi energy, which, in turn, fixes the local value of the Fermi momentum. This Fermi momentum, on the other hand, is linearly proportional to the charge density in one dimension. This is a standard reasoning behind the Thomas-Fermi description. Within this description Eq. (1) is nothing but the condition that the electrochemical potential remains constant along the NT.

The prime simplification that allows analytical solution of Eq. (1) is that, with logarithmic accuracy, $\rho(z')$ in the integrand on the right hand side (rhs) of Eq. (1) can be replaced by $\rho(z)$. Upon this replacement, we have

$$\frac{1}{e}\int_0^h dz' \mathcal{S}_0(z,z') \approx \ln\frac{h^2}{r^2} - \ln\frac{h^2}{z^2} + \ln\left(\frac{1-z/h}{1+z/h}\right), \tag{4}$$

where we assumed that $(h-z) \gg r$. With the same logarithmic accuracy, for $z \gg r$, the rhs of Eq. (4) can be replaced by $2\mathcal{L}_h$, where $\mathcal{L}_h = \ln(h/r)$. Then we obtain the following analytical solution for the induced charge density[31]

$$\rho(z) \approx \frac{gFz}{1+2g\mathcal{L}_h}, \tag{5}$$

where we have introduced a dimensionless interaction parameter $g = 2Ne^2/\pi\hbar v_0$. The above result for $\rho(z)$ is approximate, in the sense that the numerical factor in the argument of a large logarithm, $\mathcal{L}_h \gg 1$, is not specified. Equation (4) represents the solution of Eq. (1), which satisfies the obvious condition $\rho(0)=0$. An improved analytical description yielding the result coinciding with Eq. (5) in the limit of large $\mathcal{L}_h$ was recently reported in Ref. 32.

The remarkable property of the solution (5) is that the NT with poor "metallicity," $g<1$, eventually becomes metallic as the length, h, of NT is increased. This is not the case if the NT is located parallel to the conducting gate at distance $D \ll h$. In the latter case,[33,34] one has to replace $\mathcal{L}_h$ by $\ln(D/r)$.

III. THOMAS-FERMI EQUATION FOR AN ARRAY

Consider an array of parallel NTs located at points, $\mathbf{R}_i$, on the substrate (see Fig. 1). To set the Thomas-Fermi equation for a given NT, i, in the array, one has to take into account that the external potential, leading to the charge separation, contains, in addition to eFz, the potentials created by charges induced on all other NTs. Then the generalized Eq. (1) reads

$$eFz = \frac{1}{g}\rho_i(z) + \int_0^h dz' \sum_j \rho_j(z')\mathcal{S}(z,z';\mathbf{R}_i - \mathbf{R}_j), \tag{6}$$

where the kernel, $\mathcal{S}$, is given by

$$\mathcal{S}(z,z';\mathbf{R}) = \frac{1}{\sqrt{(z-z')^2+|\mathbf{R}|^2}} - \frac{1}{\sqrt{(z+z')^2+|\mathbf{R}|^2}}. \quad (7)$$

It is convenient to rewrite Eq. (6) in the "continuous" form by introducing the position-dependent density, $\rho(z,\mathbf{R})$, and the local concentration of NTs

$$\mathcal{N}(\mathbf{R}) = \sum_i \delta(\mathbf{R}-\mathbf{R}_i). \quad (8)$$

In the new notations Eq. (6) takes the form

$$eFz = \frac{1}{g}\rho(z,\mathbf{R}) + \int d\mathbf{R}'\mathcal{N}(\mathbf{R}') \times \int_0^h dz'\,\mathcal{S}(z,z';\mathbf{R}-\mathbf{R}')\rho(z',\mathbf{R}'). \quad (9)$$

The Thomas-Fermi equation in the form (9) is convenient for further analysis. This is because, as we will see below, the distributions, $\rho_i(z)$, are almost the same for *all* i even for completely random array.

IV. REGULAR ARRAY

Consider a regular array in the form of a square lattice with a lattice constant, d. Then the coordinates of $\mathbf{R}_i$ in Eq. (8) are $\{nd,md\}$ with integer m and n. Obviously, for the regular array the induced charge density, $\rho(z)$, is the same for all NTs, so that Eq. (9) acquires the form

$$eFz = \left(\frac{1+2g\mathcal{L}_d}{g}\right)\rho(z) + \int_0^h dz'\,\mathcal{S}_{ext}(z,z')\rho(z'), \quad (10)$$

where

$$\mathcal{S}_{ext}(z,z') = \sum_{\{m,n\}\neq\{0;0\}} \left(\frac{1}{\sqrt{(z-z')^2+(m^2+n^2)d^2}} - \frac{1}{\sqrt{(z+z')^2+(m^2+n^2)d^2}}\right). \quad (11)$$

Here we have isolated the self-action, $m=n=0$, of a NT. For a single NT this self-action is described by a large logarithm $\mathcal{L}_h$. In the array, however, the interaction is screened at distances $|z-z'|\gtrsim d$ by the neighboring NTs. To account for this screening, the logarithm, $\mathcal{L}_h$, in Eq. (10) is replaced by $\mathcal{L}_d = \ln(d/r)$.

It is apparent that both terms in the sum (11) diverge due to the contributions from large m,n. However, the divergent parts in both terms cancel each other. Physically, this reflects the screening by the image charges (see Fig. 1). Replacing the sums over m and n in Eq. (11) by integrals, we obtain the following expression for the kernel $\mathcal{S}_{ext}(z,z')$

$$\mathcal{S}_{ext}(z,z') = 2\pi\mathcal{N}_0(z+z'-|z-z'|) = 4\pi\mathcal{N}_0(z'\Theta(z-z')+z\Theta(z'-z)), \quad (12)$$

where $\Theta(x)$ is the step-function. Note that both steps, replacing $\mathcal{L}_h$ in Eq. (10) by $\mathcal{L}_d$ and replacing the sums in Eq. (11) by integrals, are by no means obvious and require justification. This justification is provided in the next section. In the present section we demonstrate that the integral equation (10) with the kernel (12) can be solved analytically. Upon taking the derivative from both sides of Eq. (10), we obtain

$$eF = \left(\frac{1+2g\mathcal{L}_d}{g}\right)\frac{d\rho}{dz} + 4\pi\mathcal{N}_0\int_z^h dz'\,\rho(z'). \quad (13)$$

It is now easy to see that, within a factor, the first term in Eq. (13) is the second derivative of the second term. Thus, Eq. (13) can be viewed as a second-order differential equation with respect to $\int_z^h dz'\rho(z')$. The solution of this equation, satisfying the condition $\rho(0)=0$, has the form

$$\rho(z) = \rho_0\sinh(z/a), \quad (14)$$

where ρ_0 is defined as

$$\rho_0 = \frac{eFga}{(1+2g\mathcal{L}_d)\cosh(h/a)}, \quad (15)$$

and the length, a, is given by

$$a = \frac{1}{2}\sqrt{\frac{1+2g\mathcal{L}_d}{\pi g\mathcal{N}_0}}. \quad (16)$$

The above expression for the induced charge density constitutes the main result of the present paper. It is seen from Eq. (14) that a plays the role of the penetration depth of the external field into the array. In the limit of very low density, $\mathcal{N}_0=d^{-2}\ll 1/h^2$, Eqs. (14)–(16) reproduce the result Eq. (5) for a single NT, as it could be expected, since the mutual influence of NTs, separated by a distance $\gtrsim h$, is negligible.

It also follows from Eqs. (14)–(16) that in the limit of large $\mathcal{N}_0$, such that $a\ll h$, the induced charge density is concentrated near the NT's tips and falls off towards the substrate exponentially, as $\exp[-(h-z)/a]$. This weak penetration of the external field into the array is a consequence of the collective screening. Indeed, in terms of screening properties, the array of a high density can be viewed as a homogeneous metallic plate. Our crucial observation, however, is that the penetration depth exceeds *parametrically* the lattice constant, d, both for large and small values of the interaction parameter, g.

By virtue of the relation $a/d>1$, there are *many* NTs within the penetrations depth. This, in turn, suggests that Eqs. (14)–(16) apply to the random array with average areal concentration of NTs $\mathcal{N}_0=d^{-2}$.

V. DERIVATION

In the previous section the derivation was based on two intuitive assumptions. Namely, we have assumed the self-action of a NT in the array is described by $\mathcal{L}_d$ instead of $\mathcal{L}_h$ for an isolated NT, and that the sum over m and n in Eq. (11) can be replaced by the integral. To justify these assumptions, below we calculate the sum Eq. (11) more accurately. In order to do so, we employ the following (obvious) identity. Consider a two-dimensional vector, $\mathbf{b}$, with projections b_x,b_y. Then, for arbitrary x, we have

$$\frac{1}{\sqrt{x^2+|\mathbf{b}|^2}} = \int \frac{dq_x dq_y}{2\pi}\left(\frac{\exp(-\sqrt{q_x^2+q_y^2}x)}{\sqrt{q_x^2+q_y^2}}\right) \times \exp(iq_x b_x + iq_y b_y). \quad (17)$$

To use this identity in Eq. (11), we set $b_x=nd$, $b_y=md$. Then the summation over n and m can be readily performed, yielding the sum of δ functions, i.e.,

$$\left(\frac{2\pi}{d}\right)^2 \sum_{p,l} \delta\left(q_x - \frac{2\pi p}{d}\right)\delta\left(q_y - \frac{2\pi l}{d}\right), \quad (18)$$

where p and l assume all integer values. After that the rhs in Eq. (9) acquires the form

$$\int_0^h dz' \rho(z') S(z,z'), \quad (19)$$

where $S(z,z')$ is given by

$$S(z,z') = \frac{2\pi}{d^2}(z+z'-|z-z'|) + \sum_{p,l\neq 0,0} \frac{1}{d\sqrt{p^2+l^2}} \times \left\{ \exp\left[-\left(\frac{2\pi}{d}\right)\sqrt{p^2+l^2}\sqrt{(z-z')^2}\right] - \exp\left[-\left(\frac{2\pi}{d}\right)\sqrt{p^2+l^2}\sqrt{(z+z')^2}\right]\right\}. \quad (20)$$

The first term in (20) describes the continuous limit and comes from $p=l=0$ in Eq. (18). It coincides with the kernel, $S_{ext}(z,z')$, defined by Eq. (12). The remaining sum over p and l recovers the kernel S_0 in Eq. (1). The easiest way to see this is to replace the sums over p and l by corresponding integrals, which would immediately yield $S_0(z,z')$. However, such a replacement is justified only when the large number of terms contribute to the sum. This is the case only when the condition $|z-z'|\lesssim d$ is met. For $|z-z'|\gtrsim d$ the sum over p and l in Eq. (20) is dominated by the terms $p=0$, $l=\pm 1$ and $l=0$, $p=\pm 1$, and is an *exponentially* decaying function of $|z-z'|$. This suggests that $S_0(z,z')$ should be substituted into Eq. (19), in which the integration over z' should be restricted to the interval $|z-z'|\lesssim d$. Within this interval, $\rho(z')$ in the integrand of Eq. (19) can be replaced by $\rho(z)$. The remaining integral yields $2\mathcal{L}_d = 2\ln(d/r)$, similarly to Eq. (4) with h replaced by d. The product $2\mathcal{L}_d\rho(z)$ is nothing but the first term on the rhs of Eq. (9).

The restriction of the integration interval in Eq. (19) to $|z-z'|\lesssim d$ for the part of $S(z,z')$, coming from the second term in Eq. (20), is, in fact, a delicate step. Although this part decays as $\exp(-2\pi|z-z'|/d)$ outside this interval, the behavior of $\rho(z')$ outside this interval is also exponential, namely, it increases as $\exp(z'/a)$. Therefore, the restriction of the integration interval in (19) is allowed only when the exponent in $\rho(z')$ is slower, i.e., a is $\gtrsim d$. However, we know from Eq. (16) that this is indeed the case.

VI. FLUCTUATIONS OF INDUCED CHARGE DENSITY IN A RANDOM ARRAY

The conclusion drawn in Sec. IV that the charge distribution Eq. (14) applies not only to regular but also to a random NT array was based on the relation $a>d$ between the penetration depth and the lattice constant. Thus, this conclusion pertains only to the "body" $z\sim a$ of the distribution. Since $\rho(z)$ falls off exponentially away from the NT tip, it might be expected that in the tail $(h-z)\gg a$ the randomness in NT positions would terminate the applicability of Eq. (14). To verify this fact, one can incorporate the positional disorder into Eq. (9) *perturbatively*, i.e., to find the correction to the average $\rho(z)$ linear in the fluctuation of the NT density. Then the region of applicability of Eq. (14) to the random array can be established from the condition that the *typical* disorder-induced correction is smaller than the average. This program is carried out below.

In a random array, fluctuations in the areal concentration of NTs, $\delta\mathcal{N}(\mathbf{R})=\mathcal{N}(\mathbf{R})-\langle\mathcal{N}(\mathbf{R})\rangle$, lead to the fluctuations in the distribution of the induced charge density $\delta\rho(z,\mathbf{R})$. We linearize Eq. (9) and in the first order over the fluctuations obtain

$$\hat{\mathcal{H}}\{\delta\rho(z,\mathbf{R})\} = \mathcal{F}(z,\mathbf{R}), \quad (21)$$

where the integral operator, $\hat{\mathcal{H}}$, is defined as

$$\hat{\mathcal{H}}\{f(z,\mathbf{R})\} = 4\pi\mathcal{N}_0 a^2\left(f(z,\mathbf{R}) + \frac{1}{4\pi a^2}\int d\mathbf{R}' \times \int_0^h dz' \mathcal{S}_{ext}(z,z';\mathbf{R}-\mathbf{R}')f(z',\mathbf{R}')\right). \quad (22)$$

The rhs of Eq. (21) is the potential created by the fluctuation, $\delta\mathcal{N}(\mathbf{R})$, of the density of NTs with unperturbed charge distribution, Eq. (14). As follows from Eq. (9), this potential is given by

$$\mathcal{F}(z,\mathbf{R}) = -\int d\mathbf{R}'\,\delta\mathcal{N}(\mathbf{R}')\int_0^h dz' \mathcal{S}(z,z';\mathbf{R}-\mathbf{R}')\rho(z'). \quad (23)$$

The fact that the kernel of the integral operator, $\hat{\mathcal{H}}$, depends on the difference $(\mathbf{R}-\mathbf{R}')$ suggests transformation from $\delta\mathcal{N}(\mathbf{R})$ and $\delta\rho(\mathbf{R},z)$ to the Fourier-harmonics $\delta\tilde{\mathcal{N}}(\mathbf{q})$ and $\delta\tilde{\rho}(z,\mathbf{q})$, where $\mathbf{q}$ is the in-plane wave vector. Upon the Fourier transform, Eq. (21) assumes the form

$$4\pi\mathcal{N}_0 a^2\delta\rho(z,\mathbf{q}) + \frac{2\pi\mathcal{N}_0}{q}\int_0^h dz'\,\delta\rho(z',\mathbf{q}) \times\{\exp(-|z-z'|q) - \exp[-(z+z')q]\} = \mathcal{F}(z,\mathbf{q}), \quad (24)$$

where the rhs is proportional to $\delta\tilde{\mathcal{N}}(\mathbf{q})$:

$$\mathcal{F}(z,\mathbf{q}) = \frac{4\pi a\rho_0}{q(a^2q^2-1)}\{\sinh(qz)\exp(-qh)[\cosh(h/a) + qa\sinh(h/a)] - aq\sinh(z/a)\}\delta\tilde{\mathcal{N}}(\mathbf{q}). \quad (25)$$

The structure of the kernel in Eq. (24) is similar to that in the unperturbed equation (10). It appears that, due to this similarity, Eq. (24) can be solved *analytically* in the same way as Eq. (10). Namely, upon taking the second derivative from both sides, Eq. (24) reduces to the following second-order differential equation with z-independent coefficients,

$$\delta\rho''(z,\mathbf{q}) - \gamma_q^2\delta\rho(z,\mathbf{q}) = \frac{1}{4\pi\mathcal{N}_0a^2}[\mathcal{F}''(z,\mathbf{q}) - q^2\mathcal{F}(z,\mathbf{q})], \quad (26)$$

where γ_q is defined as

$$\gamma_q^2 = q^2 + \frac{1}{a^2}. \quad (27)$$

Note that the rhs of Eq. (26) can be cast in the following simple form:

$$\mathcal{F}''(z,\mathbf{q}) - q^2\mathcal{F}(z,\mathbf{q}) = 4\pi\delta\tilde{\mathcal{N}}(\mathbf{q})\rho_0\sinh(z/a). \quad (28)$$

It can be now seen from Eq. (28) that $\lambda_q\delta\tilde{\mathcal{N}}(\mathbf{q})\sinh(z/a)$ is a particular solution of the differential equation (26). However, to find the solution of the original integral equation (24), one has to complement the particular solution with the solution of the homogeneous equation, i.e., to write

$$\delta\rho(z,\mathbf{q}) = [\chi_q\sinh(\gamma_qz) + \lambda_q\sinh(z/a)]\delta\tilde{\mathcal{N}}(\mathbf{q}) = P(z,\mathbf{q})\delta\tilde{\mathcal{N}}(\mathbf{q}), \quad (29)$$

and find the constants χ_q and λ_q by substituting Eq. (29) into Eq. (24). This yields

$$\chi_q = \frac{2\rho_0}{\mathcal{N}_0a^3q^2}\left(\frac{\cosh(h/a) + qa\sinh(h/a)}{\gamma_q\cosh(\gamma_qh) + q\sinh(\gamma_qh)}\right), \quad (30)$$

$$\lambda_q = -\frac{\rho_0}{\mathcal{N}_0a^2q^2}. \quad (31)$$

Note that λ_q diverges at small q. However, the full solution Eq. (29) remains finite in the limit $q\to 0$. It also satisfies the obvious condition $\delta\rho(0,\mathbf{q})=0$.

Equations (29)–(31) allow one to quantify the effect of disorder in the NT positions on the distribution of induced charge. The most interesting case is $h\gg a$, when this distribution is determined by collective screening involving many NTs. In this limit Eq. (29) can be simplified by replacing $\sinh(h/a)$ and $\cosh(h/a)$ by $\exp(h/a)$ and introducing $z_1 = (h-z)\ll h$. Then h drops out from the z_1-dependent part of $P(\mathbf{q})$ in Eq. (29), and we obtain

$$P(z_1,\mathbf{q}) = \frac{\rho_0e^{h/a}}{\mathcal{N}_0a^2}\times\left(\frac{\exp(-\gamma_qz_1) - \exp(-z_1/a)}{q^2} - \frac{\exp(-\gamma_qz_1)}{(q+\gamma_q)(\gamma_q+1/a)}\right). \quad (32)$$

The form (32) is very convenient to study the effect of disorder in the "tail," i.e., at large z_1. Indeed, assuming Gaussian fluctuations in $\delta\mathcal{N}(\mathbf{R})$, so that

$$\langle\delta\tilde{\mathcal{N}}(\mathbf{q}_1)\delta\tilde{\mathcal{N}}(\mathbf{q}_2)\rangle = 2\pi\mathcal{N}_0\delta(\mathbf{q}_1-\mathbf{q}_2), \quad (33)$$

the variance of random fluctuations in the induced charge density can be expressed as follows:

$$\langle\delta\rho(z_1)^2\rangle = \frac{1}{A}\int d\mathbf{R}\langle\delta\rho(z_1,\mathbf{R})^2\rangle = \frac{\mathcal{N}_0}{2\pi}\int d\mathbf{q}P(z_1,\mathbf{q})^2. \quad (34)$$

Here A is the normalization area. It is now seen that the q dependence of $P(z_1,q)$ is dominated by the first term in Eq. (32). The reason for this is the following. As was explained in the beginning of this section, the applicability of Eq. (14), obtained for the regular array, is expected to be terminated in the random array at "depths" z_1 that are $\geqslant a$. At these depths the average field is strongly suppressed. On the other hand, for $z_1>a$ one can use the expansion $\gamma_q=\sqrt{q^2+1/a^2}\simeq\frac{1}{a}+\frac{aq^2}{2}$. This, in turn, suggests that characteristic values of the wave vector, q, are $q\lesssim 1/(az_1)^{1/2}\leqslant 1/a$. Then the typical ratio of the second and the first terms in (32) is $q^2a^2\ll 1$. It also follows from the expansion of γ_q that the main exponents in $\delta\rho(z_1)$ and in the average $\rho(z_1)$ are the same. Upon neglecting the second term in Eq. (32), the q dependence of $P(z_1,q)$ acquires the form $P(z_1,q)\propto\exp(-aq^2z_1/2)/q^2$. Then the q integration in Eq. (34) can be easily performed. We will present the final result as the ratio of variance, $\langle[\delta\rho(h-z_1)]^2\rangle$, and the square of average charge density:

$$\frac{\langle[\delta\rho(h-z_1)]^2\rangle}{[\rho(h-z_1)]^2} = \frac{\ln 2}{2}\left(\frac{z_1}{\mathcal{N}_0a^3}\right). \quad (35)$$

The above result offers the quantitative answer to the question about fluctuations of the induced charge density due to the randomness in the NT positions. In particular, it can be concluded from Eq. (35) that the disorder-induced fluctuations in the charge density are negligible, if $z_1\lesssim\mathcal{N}_0a^3$. Since this value is much bigger than a, Eq. (35) confirms our earlier claim that Eq. (14) applies not only for the regular but also for the random array. However, this applicability is limited by the distance $z_1\lesssim\mathcal{N}_0a^3$. For larger z_1 the variance exceeds the average, suggesting that the charge density strongly fluctuates within the plane $z_1=$const. Note, however, that these fluctuations are smooth with characteristic scale $(z_1a)^{1/2}$, which is much smaller than z_1, but much bigger than the penetration depth, a.

As a final remark of this section, we point out that the *lower* the density of the random array, the *bigger* is the depth, z_1, down to which Eq. (14) applies, as it follows from Eq. (35). However, the *magnitude* of the decay of the charge density, $\rho(h-z_1)/\rho(h)$, is governed by the ratio z_1/a. For z_1

$=\mathcal{N}_0 a^3$, this ratio depends on the density of the array only weakly (logarithmically).

VII. IMPLICATIONS FOR FIELD EMISSION

A. Single NT

It is commonly accepted that the field emission current, J, from the NT tip is described by the Fowler-Nordheim law[35]

$$|\ln[J(F)/J_0]| = \frac{4\sqrt{2mW^3}}{3e\hbar\beta F}, \tag{36}$$

where J_0 is the prefactor, m is the electron mass, and W is the work function, which, in principle, is dependent on the tip geometry.[36–38] Parameter β is the field enhancement factor. Various applications of the field emission from NTs are based on the fact that β is large as a result of the NT geometry, more specifically, due to the large ratio h/r. The expression for the enhancement factor routinely used in fitting the experimental I-V curves[39] is $\beta = Ch/r$, where $C \sim 1$ depends on specific geometry of the tip. Within the Thomas-Fermi description of the induced charge distribution, outlined in Sec. II, the expression for field at a distance, z_1, from the NT tip is given by the derivative of the potential, $\phi(z_1)$, created by the induced charges

$$F_{ind}(z_1) = \frac{d\phi(z_1)}{dz_1} = \frac{d}{dz_1}\int_0^h dz\rho(z)S_0(z,z_1), \tag{37}$$

where $\rho(z)$ is given by Eq. (5). Then the evaluation of the integral (37) yields

$$\frac{F_{ind}(z_1)}{F} = \left(\frac{h}{2\mathcal{L}_h r}\right)\min\{1, r/z_1\}, \tag{38}$$

where we had assumed $F_{ind} \gg F$. It is seen from Eq. (38) that the enhancement factor indeed has the conventional form, $\beta = Ch/r$, with $C \approx (2\mathcal{L}_h)^{-1}$ for $z_1 \lesssim r$, but it falls off with increasing z_1. This suggests that for low enough applied fields, when the electron tunnelling length $\sim W/F_{ind}$ exceeds r, the I-V characteristics deviate from the Fowler-Nordheim law. In order to estimate this deviation, we substitute

$$\phi(z_1) = \frac{Fh}{2\mathcal{L}_h}\left(\frac{z_1}{r}\Theta(r - z_1) + [1 - \ln(r/z_1)]\Theta(z_1 - r)\right) \tag{39}$$

into the tunnelling action

$$|\ln[J(F)/J_0]| = \frac{2\sqrt{2m}}{\hbar}\int_0^{z_t} dz_1\sqrt{W - e\phi(z_1)}, \tag{40}$$

where z_t is the turning point at which the expression under the square root is zero. In (40) we had neglected the bare potential eFz_1. It is now convenient to measure the electric field in terms of F_0, defined as $F_0 = W/e\beta r = 2W\mathcal{L}_h/eh$. The integral in Eq. (40) can be reduced to the error function, $\mathrm{erf}(x)$, after which Eq. (40) acquires the form

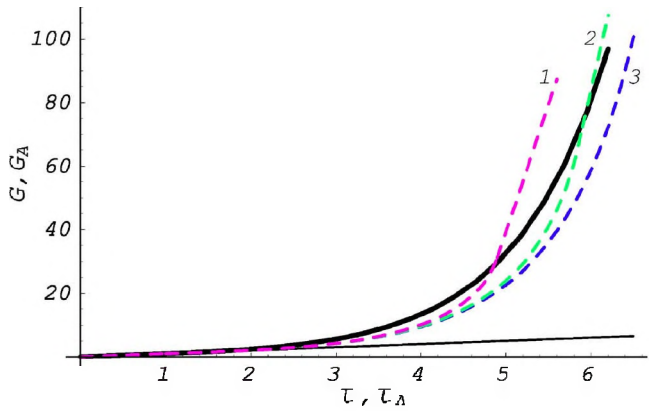

FIG. 2. (Color online) Thin solid line is the Fowler-Nordheim law $|\ln(J/J_0)| \propto \tau$, where $\tau = F_0/F$. Thick solid line is the dimensionless current-voltage characteristics $|\ln(J/J_0)|$ vs $\tau = F_0/F$ of an individual NT plotted from Eq. (42). Dashed curves 1, 2, and 3 are the current-voltage characteristics, $|\ln J|$ vs $\tau = F_A/F$ plotted from Eq. (49) for $(h/r) = 10^4$ and dimensionless array densities $\mathcal{N}_0 h^2 = 100$, 10, 1, respectively.

$$|\ln(J(F)/J_0)| = \frac{4\sqrt{2mW^3}}{3e\hbar\beta F_0}G(F_0/F), \tag{41}$$

where the dimensionless function $G(\tau)$ is defined as

$$G(\tau) = \tau, \quad \tau < 1;$$

$$G(\tau) = \tau - \left(\tau + \frac{1}{2}\right)\left(1 - \frac{1}{\tau}\right)^{1/2} + \frac{3}{4}\sqrt{\frac{\pi}{\tau}}\exp(\tau - 1)\mathrm{erf}(\sqrt{\tau - 1}), \quad \tau > 1. \tag{42}$$

The plot of the function $G(\tau)$ is shown in Fig. 2. Strictly speaking, the Fowler-Nordheim region corresponds to $\tau < 1$, where the slope of $G(\tau)$ is identically unity. However, $G(\tau)$ can be linearized around $\tau > 1$, where the slope is larger. For example, at $\tau = 2$ the slope is ≈ 2. This can be interpreted as a two-times reduction of the enhancement factor, β, in Eq. (41). A significant reduction of the enhancement factor (e.g., 30 times) occurs around $\tau \approx 5$. It should be noted that since Eqs. (41) and (42) were derived neglecting the bare potential, their applicability is limited by $\tau < \tau_{max}$, where τ_{max} corresponds to the applied field $F = F_0/\tau_{max}$, for which the turning point, z_t, in the tunnelling action Eq. (40) reaches the value W/F. The latter condition can be rewritten in the form $(\tau_{max} - 1) = \ln(h\tau_{max}/r)$, yielding $\tau_{max} \approx \ln(h/r) = \mathcal{L}_h$. For $\tau > \tau_{max}$, i.e., for applied fields $F > F_0/\tau_{max}$, the I-V characteristics is given by the Fowler-Nordheim law (36) with $\beta = 1$.

Overall, Fig. 2 indicates that for low enough applied fields there are significant deviations from the Fowler-Nordheim law in the I-V characteristics of an individual NT. For such fields the linearity of the Fowler-Nordheim plots shows only within a very narrow interval of F. On the experimental side, there are reports, e.g., Ref. 40, where applicability of the Fowler-Nordheim law was demonstrated within a rather wide (exceeding three times) interval of change of F. In

other reported measurements, see, e.g., Ref. 41, linearity of $\ln J$ vs. $1/F$ holds only within a limited (less than two times) interval of applied fields. Whether or not Eq. (41), derived for a single NT, is suitable to fit experimental results depends crucially on the *geometry* of the array, as we discuss below.

B. Array of NTs

As it was mentioned in the Introduction, increasing the density of NTs in the array leads to dramatic suppression of the enhancement factor. To illustrate this point, consider first the array of low density, when the tunnelling length is much smaller than the distance between the neighboring NTs. Then the field created by induced charges near the tip of a given NT can be calculated from Eq. (37), with $\rho(z)$ given by Eqs. (14) and (15). This calculation yields the generalization of the field enhancement factor Eq. (38) to the case of the array of low density:

$$\frac{F_{ind}(z_1)}{F} = \left[\frac{a}{2r\mathcal{L}_d}\tanh\left(\frac{h}{a}\right)\right]\min\{1, r/z_1\}. \tag{43}$$

The above expression recovers the enhancement factor for a single NT in the limit $a \to \infty$ or equivalently, $\mathcal{N}_0 \to 0$. For $a < h$, we conclude that the enhancement factor for the array, compared to the single NT, is suppressed as

$$\frac{\beta(\mathcal{N}_0)}{\beta(0)} = \frac{a\mathcal{L}_h}{h\mathcal{L}_d} = \left(\frac{\mathcal{L}_h^2}{2\pi\mathcal{L}_d\mathcal{N}_0 h^2}\right)^{1/2} \ll 1. \tag{44}$$

We now turn to the high-density array. In such an array, the tunnelling length of an emitted electron can exceed the distance, $\mathcal{N}_0^{-1/2}$, between the neighboring NTs. Then the form of the tunnelling barrier is no longer given by the potential created by a single NT with charge distribution modified by neighboring NTs. Instead, one has to use a general expression

$$\phi_A(z_1) = \int_0^h dz\, \rho_0 \sinh[(h-z)/a]\mathcal{S}(z, z_1), \tag{45}$$

where $\mathcal{S}$ is the kernel defined by Eq. (20). The first term in the kernel (20) corresponds to the "continuous" limit and yields a contribution Fz_1 to $\phi_A(z_1)$. The second term in Eq. (20) exhibits different behavior for large ($|z-z_1| \gg \mathcal{N}_0^{-1/2}$) and small ($|z-z_1| \ll \mathcal{N}_0^{-1/2}$) distances. The expression for $\phi_A(z_1)$ that captures both long- and short-distance behaviors has the form

$$\phi_A(z_1) = Fz_1 + \frac{Fd}{2\sqrt{2\mathcal{L}_d}}\left\{\frac{a\Theta(z_1-d)}{2\pi a + d}\left[\exp\left(-\frac{2\pi z_1}{d}\right) - 1\right] + \Theta(d-z_1)\ln\left(\frac{d}{z_1}\right)\exp\left(-\frac{z_1}{a}\right)\right\}. \tag{46}$$

The long-distance behavior is described by the first term in the square brackets. It represents the correction to the "continuous" first term, Fz_1, in (46) due to discreteness of the array. Clearly, the field enhancement due to this term is negligible. It is the second term in the square brackets that is responsible for the field enhancement. The physics, captured by this term, is that at distance $z_1 < \mathcal{N}_0^{-1/2}$ the tunnelling electron "sees" not only the NT, from which it was emitted, but also neighboring NTs. This term, however, does not contain the NT radius, r, which was set to zero in the derivation of Eq. (46). The dependence on r can be reinstated in the same way as for a single NT in Eq. (39), namely

$$\phi_A(z_1) \approx \frac{Fd}{2\sqrt{2\mathcal{L}_d}}\left\{\Theta(r-z_1)\frac{z_1}{r} + \Theta(z_1-r)\Theta(d-z_1) \times\left[1 - \ln\left(\frac{r}{z_1}\right)\right]\exp(-[z_1-r]/a)\right\}, \tag{47}$$

where we have retained only the part responsible for the field enhancement. The subsequent calculation of *I-V* characteristics using Eq. (47) is completely identical to the case of an isolated NT. The result can be presented in the form similar to Eqs. (41) and (42)

$$|\ln[J(F)/J_0]| = \frac{4\sqrt{2mW^3}}{3e\hbar\beta(\mathcal{N}_0)F_A}G_A(F_A/F), \tag{48}$$

$$G_A(\tau) = \tau\left[1 - \left(1 - \frac{1}{\tau}\right)^{3/2}\right] + \frac{1}{\sqrt{\tau}}\int_1^{u_\tau} du\left[(1+\ln u_\tau) \times\exp\left(-\frac{r}{a}(u_\tau - 1)\right) - (1+\ln u)\exp\left(-\frac{r}{a}(u-1)\right)\right], \tag{49}$$

where u_τ, which is related to the turning point, z_τ, as $u_\tau = z_\tau/r$, satisfies the following equation:

$$\tau = (1+\ln u_\tau)\exp\left(-\frac{r}{a}(u_\tau - 1)\right). \tag{50}$$

The boundary value of the external field, F_A, corresponds to the turning point $z_\tau = (F_A/F)r = \tau_A r \geq r$. The field F_A is related to the single NT boundary field, F_0, by

$$F_A = \frac{\mathcal{L}_d h}{\mathcal{L}_h a}F_0. \tag{51}$$

Therefore, the variable, τ_A, defined above, is related to the corresponding single NT variable, τ, as

$$\tau_A = \left(\frac{2\pi\mathcal{L}_d\mathcal{N}_0 h^2}{\mathcal{L}_h^2}\right)^{1/2}\tau. \tag{52}$$

The function $G_A(\tau_A)$ is plotted in Fig. 2 together with the function $G(\tau)$. We see that while the parameter $\mathcal{N}_0 h^2$ changes within a wide interval, the function $G(\tau_A)$ remains close to $G(\tau)$. This means that the *form* of the *I-V* characteristics for the array is similar to that for a single NT. The difference essentially amounts to rescaling of the characteristic field, F_0, by the factor $\mathcal{L}_d h/\mathcal{L}_h a$. In other words, increasing the density of the array results in suppression of the field emission without the change of the shape of the *I-V* characteristics. It should be pointed out that this conclusion pertains to the array of randomly positioned, but completely *identical*, NTs. As we will see below, the situation changes dramatically when the heights of NTs are random.

VIII. DISCUSSION AND CONCLUDING REMARKS

The main result of the present paper is Eq. (14) that describes the crossover of the induced charge density distribution from a single NT to the dense regular array of NTs. We have also demonstrated that Eq. (14) applies to the random array. Disorder in the NT positions terminates the applicability of Eq. (14) only at large distances from the tips, where the charge density had already dropped significantly. Concerning the field emission, our calculations quantify a strong suppression of the emission current in a dense array. The field enhancement factor falls off with the NT density, $\mathcal{N}_0$, as $\mathcal{N}_0^{-1/2}$ [see Eq. (44)]. This conclusion might seem to contradict the majority of experiments, where high enhancement factors for dense arrays were reported. More precisely, in the majority of experiments the dependence of emission current on the NT density is simply not addressed, and the *I-V* characteristics are interpreted basing on the properties (such as work-function) of individual NTs. In fact, in those few papers where this issue is addressed, the suppression of field emission with increasing the NT density is pointed out on a *qualitative* level. The resolution of this contradiction, in our opinion, lies in the fact that in realistic situations the heights of NTs in the array are *widely dispersed*. To get an insight how this dispersion in heights affects the field emission, consider a regular array in which one NT is higher than others by h_1, which is much larger than the average NT separation, $\mathcal{N}_0^{-1/2}$, but much smaller than h. Within the interval $0<z<h$ the distribution of charge in this "sticking out" NT is "enforced" by the neighbors and is given by Eqs. (14)–(16). However, within the interval $h<z<(h+z_1)$ this NT "sees" the rest of the array as an equipotential plane. From this observation we immediately conclude that, within the interval $h<z<(h+z_1)$, the charge density in the sticking out NT is given by Eq. (5) with z replaced by $(z-h)$. This, in turn, suggests that the enhancement factor of the external field in the sticking out NT is high and is equal to $h_1/2\mathcal{L}_{h_1}r$, as follows from Eq. (38).

The above reasoning suggests that the conjecture that the field emission current is dominated by sparse sticking out NTs allows us to account for the high values of the enhancement factor observed in the experiment. We will now demonstrate that this conjecture also allows us to explain why the dependence $\ln[J(F)/J_0]$ follows the Fowler-Nordheim law (36) within a wide interval of F, while Eqs. (41) and (42) predict strong deviations from Eq. (36) as F is decreased.

Obviously, the probability, $P(h_1)$, to find within the array a NT that sticks out by h_1 *decreases* with h_1. Contribution of NTs with given h_1 to the emission current is determined by the product

$$J_{h_1} \propto \exp\{[-4(2mWr^2)^{1/2}/3\hbar]G(F_0/F)\}P(h_1), \quad (53)$$

where the first term is the tunnelling action, which depends on h_1 through $F_0=2W\mathcal{L}_{h_1}/eh_1$; the function G is defined by Eq. (42). Since the tunnelling action *increases* rapidly with h_1, the product (53) has a sharp maximum at a certain optimal h_1. Therefore, $\ln[J(F)/J_0]$ is determined by the logarithm of the rhs of Eq. (53) taken at optimal h_1. The natural choice for $P(h_1)$ is the Poisson distribution, $\exp(-h_1/H)$. We can also use the fact that within the interval $2<\tau<10$ the function $G(\tau)$ can be approximated with high accuracy by the power law

$$G(\tau) \approx 0.23\tau^{9/2}. \quad (54)$$

Using this approximation, the optimal h_1 can be easily found analytically. It is convenient to cast the final result for $\ln[J(F)/J_0]$ in the following form

$$|\ln[J(F)/J_0]| = \left(\frac{4\sqrt{2mW^3}}{3e\hbar\beta_H F}\right)^{9/11}, \quad (55)$$

where the "effective" enhancement factor is defined as

$$\beta_H = 4.8\frac{H}{r\mathcal{L}_H}\left(\frac{2mr^2W}{\hbar^2}\right)^{7/18}. \quad (56)$$

First, we see from Eq. (55) that the *I-V* characteristics are very close to the Fowler-Nordheim law, since the exponent 9/11 is close to 1. This should be contrasted to the *I-V* characteristics of a single NT, for which $|\ln[J(F)/J_0]| \propto F^{-9/2}$, as follows from Eq. (54). Secondly, the effective enhancement factor (56) is large and depends rather weakly on the work function W. Summarizing, the dense array of NTs can exhibit the Fowler-Nordheim field emission provided there is a sufficient spread in the NT heights. In fact, this conclusion is in accord with reported experimental findings. In particular, direct imaging of emission intensity by means of scanning[41,42] and electron emission[43,44] microscopy reveals that only a tiny portion of NTs (10^{-4} or even smaller) contributes to the net current.

ACKNOWLEDGMENTS

This work was supported by NSF under Grant No. DMR-0503172 and by the Petroleum Research Fund under Grant No. 43966-AC10.

[1] A. G. Rinzler, J. H. Hafner, P. Nikolaev, L. Lou, S. G. Kim, D. Tomanek, P. Nordlander, D. T. Colbert, and R. E. Smalley, Science **269**, 1550 (1995).

[2] P. G. Collins and A. Zettl, Appl. Phys. Lett. **69**, 1969 (1996).

[3] Q. H. Wang, A. A. Setlur, J. M. Lauerhaas, J. Y. Dai, E. W. Seelig, and R. P. H. Chang, Appl. Phys. Lett. **72**, 2912 (1998).

[4] K. Okano, T. Yamada, H. Ishihara, S. Koizumi, and J. Itoh, Appl. Phys. Lett. **70**, 2201 (1997).

[5] J. S. Lee, K. S. Liu, and I. N. Lin, Appl. Phys. Lett. **71**, 554 (1997).

[6] Y. Chen, S. Patel, Y. Ye, D. T. Shaw, and L. Guo, Appl. Phys. Lett. **73**, 2119 (1998).

[7] Q. H. Wang, A. A. Setlur, J. M. Lauerhaas, J. Y. Dai, E. W. Seelig, and R. P. H. Chang, Appl. Phys. Lett. **72**, 2912 (1998).
[8] Q. H. Wang, M. Yan, and R. P. H. Chang, Appl. Phys. Lett. **78**, 1294 (2001).
[9] H. Araki, T. Katayama, and K. Yoshino, Appl. Phys. Lett. **79**, 2636 (2001).
[10] C. J. Lee, T. J. Lee, S. C. Lyu, Y. Zhang, H. Ruh, and H. J. Lee, Appl. Phys. Lett. **81**, 3648 (2002).
[11] H. Jia, Ye Zhang, X. Chen, J. Shu, X. Luo, Z. Zhang, and D. Yu, Appl. Phys. Lett. **82**, 4146 (2003).
[12] R. H. Baughman, A. A. Zakhidov, and W. A. de Heer, Science **297**, 787 (2002).
[13] S. Fan, M. G. Chapline, N. R. Franklin, T. W. Tombler, A. M. Cassell, and H. Dai, Science **283**, 512 (1999).
[14] See, e.g., http://www.xintek.com/products/
[15] M. Chhowalla, C. Ducati, N. L. Rupesinghe, K. B. K. Teo, and G. A. J. Amaratunga, Appl. Phys. Lett. **79**, 2079 (2001).
[16] J. S. Suh, K. S. Jeong, J. S. Lee, and I. Han, Appl. Phys. Lett. **80**, 2392 (2002).
[17] H. J. Lee, S. I. Moon, J. K. Kim, Y. D. Lee, S. Nahm, J. E. Yoo, J. H. Han, Y. H. Lee, S. W. Hwang, and B. K. Ju, J. Appl. Phys. **98**, 016107 (2005).
[18] Ch. Adessi and M. Devel, Phys. Rev. B **62**, R13314 (2000).
[19] S. Han, M. H. Lee, and J. Ihm, Phys. Rev. B **65**, 085405 (2002).
[20] A. Mayer, N. M. Miskovsky, and P. H. Cutler, Phys. Rev. B **65**, 155420 (2002).
[21] G. Zhou and Y. Kawazoe, Phys. Rev. B **65**, 155422 (2002).
[22] S. Han and J. Ihm, Phys. Rev. B **66**, 241402(R) (2002).
[23] S.-D. Liang and N. S. Xu, Appl. Phys. Lett. **83**, 1213 (2003).
[24] A. Buldum and J. P. Lu, Phys. Rev. Lett. **91**, 236801 (2003).
[25] X. Zheng, G. Chen, Z. Li, S. Deng, and N. Xu, Phys. Rev. Lett. **92**, 106803 (2004).
[26] S.-D. Liang, N. Y. Huang, S. Z. Deng, and N. S. Xu, Appl. Phys. Lett. **85**, 813 (2004).
[27] J. Peng, Z. Li, C. He, S. Z. Deng, N. S. Xu, X. Zheng, and G. Chen, Phys. Rev. B **72**, 235106 (2005).
[28] This is the consequence of the fact that the induced charge density depends very weakly (logarithmically) on the NT cross section, πr^2. Then, two sufficiently close NTs can be viewed as a single NT with cross section $2\pi r^2$.
[29] L. Nilsson, O. Groening, C. Emmenegger, O. Kuettel, E. Schaller, L. Schlapbach, H. Kind, J.-M. Bonard, and K. Kern, Appl. Phys. Lett. **76**, 2071 (2000).
[30] H. M. Manohara, M. J. Bronikowski, M. Hoenk, B. D. Hunt, and P. H. Siegel, J. Vac. Sci. Technol. B **23**, 157 (2005).
[31] E. G. Mishchenko and M. E. Raikh, cond-mat/0507115 (unpublished).
[32] Z. Li and W. Wang, cond-mat/0603509 (unpublished).
[33] K. A. Bulashevich and S. V. Rotkin, JETP Lett. **75**, 205 (2002).
[34] S. Sapmaz, Ya. M. Blanter, L. Gurevich, and H. S. J. van der Zant, Phys. Rev. B **67**, 235414 (2003).
[35] R. H. Fowler and L. W. Nordheim, Proc. R. Soc. London, Ser. A **119**, 173 (1928).
[36] G. Zhou, W. Duan, and B. Gu, Phys. Rev. Lett. **87**, 095504 (2001).
[37] Ji Luo, L.-M. Peng, Z. Q. Xue, and J. L. Wu, Phys. Rev. B **66**, 155407 (2002).
[38] S. Han and J. Ihm, Phys. Rev. B **66**, 241402(R) (2002).
[39] See, e.g., the most recent papers J. M. Bonard, K. A. Dean, B. F. Coll, and C. Klinke, Phys. Rev. Lett. **89**, 197602 (2002); J. Y. Huang, K. Kempa, S. H. Jo, S. Chen, and Z. F. Ren, Appl. Phys. Lett. **87**, 053110 (2005); A. L. Musatov, K. R. Izrael'yants, A. B. Ormont, A. V. Krestinin, N. A. Kiselev, V. V. Artemov, O. M. Zhigalina, and Yu. V. Grigoriev, *ibid.* **87**, 181919 (2005); J. C. She, S. Z. Deng, N. S. Xu, R. H. Yao, and J. Chen, *ibid.* **88**, 013112 (2006); N. S. Ramgir, I. S. Mulla, K. Vijayamohanan, D. J. Late, A. B. Bhise, M. A. More, and D. S. Joang, *ibid.* **88**, 042107 (2006); B. Wang, Y. H. Yang, C. X. Wang, N. S. Xu, and G. W. Yang, *ibid.* **98**, 124303 (2005).
[40] O. Gröning, O. M. Küttel, Ch. Emmenegger, P. Gröning, and L. Schlapbach, J. Vac. Sci. Technol. B **18**, 665 (2000).
[41] J.-M. Bonard, K. A. Dean, B. F. Coll, and C. Klinke, Phys. Rev. Lett. **89**, 197602 (2002).
[42] V. I. Merkulov, D. H. Lowndes, and L. R. Baylor, J. Appl. Phys. **89**, 1933 (2001).
[43] S. Gupta, Y. Y. Wang, J. M. Garguilo, and R. J. Nemanich, Appl. Phys. Lett. **86**, 063109 (2005).
[44] H. J. Lee, Y. D. Lee, W. S. Cho, B. K. Ju, Y.-H. Lee, J. H. Han, and J. K. Kim, Appl. Phys. Lett. **88**, 093115 (2006).